OPTICAL REVIEW Vol. 20, No. 5 (2013) 433–437

Experimental Investigation of a Flowing Fluid Layer on Metal Surface Roughness Measurement and Aberration Correction Using Adaptive Optics

Yiin Kuen FUH* and Jia Ren FAN

Institute of Opto-mechatronics Engineering, National Central University, Jhongli, Taoyuan 32001, Taiwan

(Received April 23, 2013; revised June 7, 2013; Accepted June 10, 2013)

The induced optical aberration of laser beam passing through a transparent flowing fluid layer on a metal specimen is experimentally and empirical formula studied. The proposed study presents an experimental investigation of metal surface roughness measurement by combining an optical probe of laser-scattering phenomena and adaptive optics (AO) for aberration correction. In the absence of the AO correction scheme, induced flow velocity of 0.278 m/s can severely degrade the residual wavefront root mean square (RMS) error to 0.58 μm and decrease the scattered laser intensity. Real-time AO correction in closed-loop at a sampling rate of 8 Hz can reduce the wavefront RMS error to 0.19 μm and improve the attenuation of scattered laser intensity. The maximum relative error of the estimated roughness (R_a) is less than 7.8% compared with the stylus method. The experimental results show satisfactory correction in the presence of a flowing fluid layer using the AO system.

Keywords: adaptive optics, scattering, surface roughness

1. Introduction

Adaptive optics (AO) are originally designed and employed in astronomy to compensate for atmospheric turbulence, which is the crucial limiting factor for the performance of ground-based telescopes.[1,2] Latest progresses aim to develop large stroke and out-of-plane actuators for driving segmented mirrors in very large astronomical telescopes such as giant magnetostrictive and compliant thermal actuators.[3,4] This technology is also capable of improving and correcting ocular as well as higher-order aberrations such that in vivo imaging of the retina in vision science can be drastically improved.[5–7] Moreover, AO is recently deployed in the non-contact type measurement of specimen surface roughness.[8,9] For example, a simple yet powerful measuring device that integrates AO and light scattering method have been proposed and an improved version of AO-assisted system for measuring the surface roughness in situ under dynamic air turbulence was lately reported,[10] above integrated systems of adaptive optics have demonstrated to be the effective in measuring surface roughness of metals. In addition to the disturbances of air flow, the coolant fluid applied at the machining zone during various operations such as grinding, milling etc. is another dominant factor to the measuring accuracy. Due to the inherent opaque property and free running surface of the coolants, an inaccessible problem for in-process optical measurement of specimen surface quality will be encountered.[11] A transparent window method was proposed to produce an optical clean zone on the specimen surface.[12] Furthermore, an applicator was theoretically modeled and incorporated into the Beckmann–Kirchhoff scattering theory.[13] The effect of additional clean fluid layers and the associated accuracy of surface roughness measurement has been theoretically calculated and the deflection of the laser beam caused by fluid flow was found to be negligible. However, researchers have not investigated the optical aberrations and scattered laser power attenuation induced by a flowing fluid layer experimentally and theoretically. To address this issue, we also employ a similar apparatus in[14,15] and examine the aberrations induced by above-mentioned flowing fluid at various velocities. In what follows the experimental results indicate that real-time AO can correct both static and dynamic phase distortions induced by flowing fluid effectively. Therefore, an experimental facility has been employed in our in-process AO-assisted optical measurement of surface roughness considering one transparent flowing fluid layer.

2. Experiment

2.1 *Laser beam reflecting and scattering detection system*

When a coherent light source is projected onto a rough surface, the reflected laser pattern image is a result of the composite effects of interference and scattering. The relationship between the power of the reflected laser and surface roughness can be used to measure surface roughness.[16] We have developed an in process measuring device for rapid surface roughness measurement and the same device is applied here.[10] Figure 1 shows a structural diagram of surface roughness measuring device in the presence of a flowing fluid layer. The overall structure consists of a laser beam reflecting and scattering detection system, a simple fluid-supporting system and a real-time AO compensating system. *Laser beam reflecting and scattering detection system* comprises a power meter connects with a sensor, beam splitters and a measuring lens. The incident light is a collimated He–Ne laser (output of 5 mW, wavelength of 633 nm) served as the probe laser. The laser beam projected onto the specimen surface along the normal direction by a beam splitter. The peak power of scattered

*E-mail address: mikefuh@ncu.edu.tw

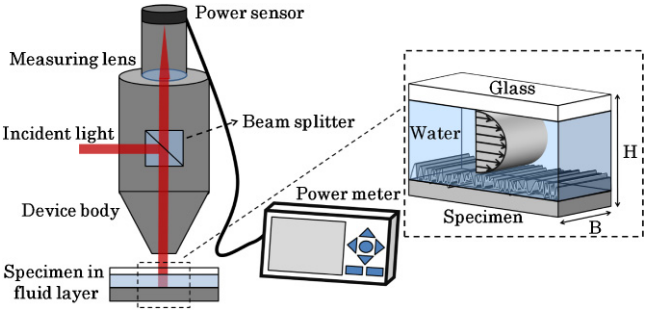

Fig. 1. (Color online) Schematic structure of the measuring device. Inset is the transversal section of the specimen immersed in a flowing fluid layer and laminar velocity profile is illustrated.

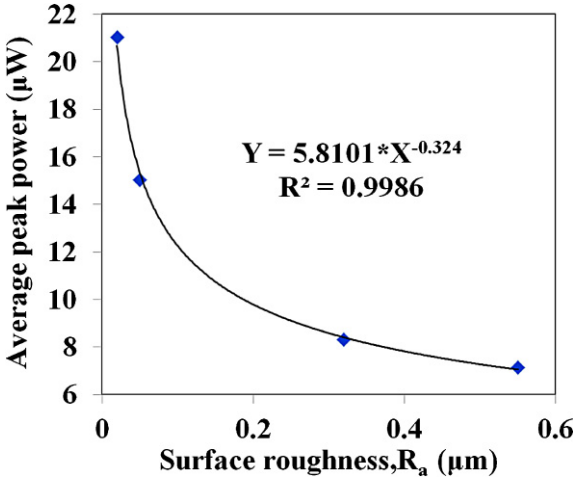

Fig. 2. (Color online) The correlation between the reflected average laser peak power and surface roughness (R_a). The specimens were immersed in a static water layer.

laser beam from the specimen surface, which is immersed in flowing water layer in a rectangular container and covered with a glass, was focused on the optical power sensor through a measuring lens (focus length 50 mm) and recorded in real time by an optical power meter (Thorlabs PM100D).

2.2 *Characteristics of a flowing fluid layer*

As described above, the transparent flowing fluid layer on specimen surface is the main research objective in our study. Flow characterization of different regimes for laminar or turbulent can be experimentally related to the Reynolds number, *Re*. A critical value of the Reynolds number is typically used to define the transition from laminar to turbulent flows. The dimensionless Reynolds number is defined as

$$Re = VRv^{-1}, \tag{1}$$

where R is hydraulic radius ($R = AP^{-1}$, where A is the cross-sectional area and P is the wetted perimeter), V is the characteristic flow velocity and v is the kinematic viscosity of the flowing fluid. In this paper, rectangular section is used and the flow velocity is in the range of 0–0.278 m/s. The width of the cross section B is 80 mm, the distance between the glass plate and the surface H is 15 mm and water kinematic viscosity $v = 1.01\,\mathrm{mm}^2/\mathrm{s}$. It is calculated that for the condition $V = 0$–$0.278\,\mathrm{m/s}$, the related Reynolds number is $Re = VR/v = VA/(Pv) = VBH/[2v(B + H)] = 0$–$1738$. The flow regime used in this experiment is predicted to be a laminar flow since the critical value of the Reynolds number is below the critical value. Therefore, the laminar flow velocity profile can be seen in inset of Fig. 1, which shows the transversal section of the surface with additional fluid layer and corresponding parabolic velocity profile.

Theoretically, flowing fluid flow would inevitably lead to light deviation and is the major distinction between the static and the dynamic aberrations. The incident, reflected and scattered laser beams as well as the deflection can be computed by the following method[15] such that the deflection of the laser beam, l, when they pass through the flowing fluid layer can be deduced and approximated as

$$l = \frac{VH}{c} \times \left(\frac{2}{3}\right). \tag{2}$$

The effect of the propagation of the laser beam through the flowing fluid layer can be evaluated. Substituting $V = 0.278\,\mathrm{m/s}$, $H = 0.015\,\mathrm{m}$, and $c = c_0 n_2^{-1} = 2.25 \times 10^8\,\mathrm{m/s}$ into this equation, where c_0 is the velocity of light in vacuum and n_2 is the refractive index of water, l is calculated as $1.236 \times 10^{-5}\,\mu\mathrm{m}$. Therefore, the calculated deflection of the laser beam through the flowing fluid layer is small under the given conditions.

On the other hand, even the calculated light deflection is small, however, it is experimentally proved in next two sections that this flowing fluid will result in the inaccuracy of surface roughness measurement in a typical optical scattering method.

2.3 *The regression curve of surface roughness and scattered light intensity for the static fluid*

Previous researches have shown that there is a good correlation existed between the scattered light intensity and surface roughness R_a routinely achieve less than 10% error values.[17–19] Figure 2 shows the correlation between the average reflected laser peak power and surface roughness R_a, the specimens were immersed in a static water layer ($V_0 = 0$) were flat steels with known surface roughness of R_a values 0.02, 0.05, 0.32, and 0.55 μm, respectively. The specimens were mechanically polished with a lapping fixture using different grades of sandpapers and R_a values were determined by stylus method (ACCRETECH Surfcom 130A). In Fig. 2, the laser beam intensity decreases with an increase of the surface roughness owing to the scattering effect. The experimentally measured scattering laser intensity change with surface roughness can be fitted with a curve, and the numerically calculated result was expressed as follows

$$Y = 5.8101 \times X^{-0.324}, \quad R^2 = 0.9986, \tag{3}$$

where Y is the scattered laser power intensity, X is the surface roughness, and R^2 is the coefficient of correlation.

Table 1. Correlation formula and calculated results for surface roughness values in static and two flow velocities.

	R_a (μm)			
	0.02	0.05	0.32	0.55
Peak power of $V_0 = 0$	21.0175	15.0295	8.3255	7.1532
Peak power of $V_1 = 0.167$ m/s	20.5980	14.6483	7.7823	6.5115
R_a I [Eq. (3)]	0.0201	0.0576	0.4058	0.7035
Relative error of R_a (%)	0.64	1.53	26.81	27.91
Peak power of $V_2 = 0.278$ m/s	20.3778	14.3682	7.5184	6.2037
R_a II [Eq. (3)]	0.0208	0.0612	0.4514	0.8169
Relative error of R_a (%)	4.04	22.34	41.06	48.52

Note: R_a I and R_a II are the estimated value of R_a by Eq. (3).

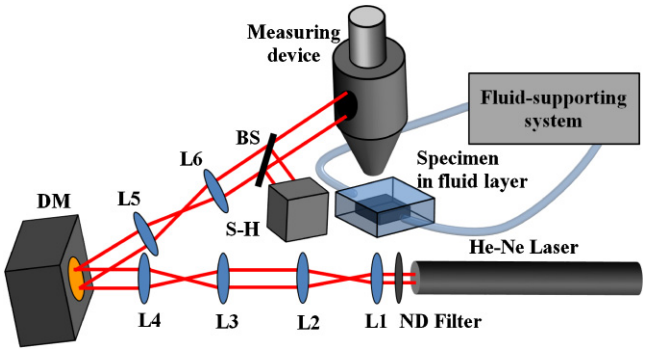

Fig. 3. (Color online) Schematic diagram of the experimental setup with adaptive optics system.

2.4 *Adaptive optics system*

In order to better understand and solve the problem of measuring error caused by the flowing fluid layer and associated attenuation of laser beam intensity, we introduce the AO system to correct the optical aberrations in real time to improve measuring precision. Figure 3 shows a schematic diagram of the experimental setup. He–Ne laser beam was used was used as a light source. The laser beam was collimated and expanded by a pair of lenses (L1 and L2, having focal lengths of 50 and 150 mm, respectively) with a magnification factor of 3. Then passed through another pair of relay lenses (L3 and L4, each with a focal length of 75 mm) and irradiated on a deformable mirror (DM; Boston Micromachines Multi-DM-UM01). The DM, which has 140 actuators, served as a correction device. The laser beam reflected by the DM then passed through another pair of lenses (L5 and L6, each with a focal length of 75 mm). The light entered into the measuring device and reflected by a BS (beam splitter), which was assembled inside the device to illuminate the specimen surface, and the illuminated area is approximately 3 mm^2. Finally the reflected light from specimen surface passed through the flowing fluid layer and projected onto the Shack–Hartmann wavefront sensor (S–H; Thorlabs WFS150C) by another BS.

In addition, the fluid-supporting system is designed to simulate the flowing fluid effect. It consists of a pump, tank, flow meter, pipes and an observing chamber for specimen immersed in fluid layer. The proposed system is capable of recording the scattered light intensity and correcting the optical aberrations induced by flowing fluid in real time.

2.5 *The optical aberration in the presence of a flowing fluid layer*

Four known R_a specimens were used to experimentally investigate the effect of fluid layer with different flow velocities. The results in Table 1 clearly showed that the increase of water flow velocity, the average peak power of scattered laser beam was attenuated. In the cases of flow velocity of 0.167 m/s and specimens roughness values of 0.32 and 0.55 μm, the attenuated light of peak power intensity were experimentally measured to be 7.7823 and 6.5115, respectively, as compared with the static values of 8.3255 and 7.1532. The differences of attenuation are even significant as the flow velocity increases to 0.278 m/s, the measured attenuated light were 7.5184 and 6.2037, respectively. Moreover, the estimated R_a based on regression formula for flow velocity $V_1 = 0.167$ and $V_2 = 0.278$ m/s have profoundly differences from the static condition ($V_0 = 0$). This impact is especially noticeable in rough surfaces 0.32 and 0.55 μm, the relative errors of calculated R_a are 41.06 and 48.52%, respectively. This will severely degrades the measuring accuracies for surface roughness by optical scattering measurement and AO correction is proposed to mitigate this problem.

3. Results and Discussion

3.1 *Characterization of metal surface immersed in fluid*

Figure 4(a) shows the measured average peak power of four specimens in static and flow velocities of 0.167 and 0.278 m/s, respectively. It is demonstrated that the faster flow velocity produces more evident peak power attenuation and fluctuation. Here we take the specimen of $R_a = 0.02$ μm and the recorded peak power as a function of measured time for different flow velocities as shown in Fig. 4(b). According to this figure, the variation of peak power is primarily affected by the flow velocity, and with the increase of flow velocity from 0 to 0.278 m/s, the fluctuation of peak power also increase from 0.15 to 6.92%. This will inevitably result in measurement errors and regression formula based on light scattering cannot be reliably used in the presence of a flowing fluid layer. Therefore, we use the AO system to sense and correct aberrations in real time.

3.2 *Wavefront correction by AO system and gain effect*

Figure 5 shows the average wavefront RMS error and variations in a closed-loop AO system considering the

effects of different gains. The experiments were conducted using the specimen R_a 0.02 μm and the flow velocity 0.278 m/s. The AO control system is implemented by governing the amplitude of the DM adjustment vector to calculate the wavefront correction,[20] the change of different gains will have an effect on how fast and accurate the wavefront will correct itself, and experimentally the threshold gain of 500 can reach minimal oscillation of the RMS amplitude and magnitude.

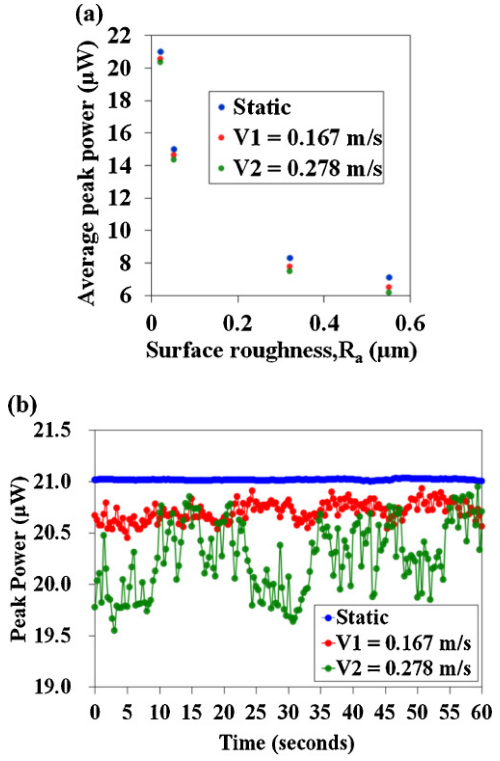

Fig. 4. (Color online) (a) Measured average peak power of four specimens in three different flow velocities. (b) Peak power as a function of measured time for different flow velocities in fluid layer for the specimen with $R_a = 0.02$ μm.

Figure 6 shows the function of Zernike coefficients for the 15th polynomials with and without the AO system. Again, specimen R_a 0.02 μm and the flow velocity 0.278 m/s were used in these experiments. The wavefront map degrades immensely because of flowing fluid layer, and the peak to valley (P–V) and RMS values are ~2.28 and ~0.58 μm, respectively. With AO system correction, the temporal average residual aberration causes P–V and RMS errors of ~0.91 and ~0.19 μm, respectively. This is 70% reduction in overall wavefront errors. Furthermore, the AO-corrected coefficient values are experimentally found to be more effective in correcting lower-order aberrations. For example, the Z1–Z5 values are 0.043, 0.09, 0.015, 0.004, and 0.036 μm, respectively, with a closed-loop AO system. The AO improvement is less significant in higher-order aberrations because the original aberrations without AO correction already have smaller Zernike coefficients.

The AO-assisted system can remarkably reduce the aberrations caused by the flowing fluid layer. Moreover, the attenuation of scattered laser beam can be minimized in the faster flow velocity condition and the proposed AO system has good correction performance as shown in Table 2. The corrected laser peak powers of $V_2 = 0.278$ m/s in four different specimens all have efficacious improvement such that relatively closed to the original value of static condition can be obtained. The relative surface roughness

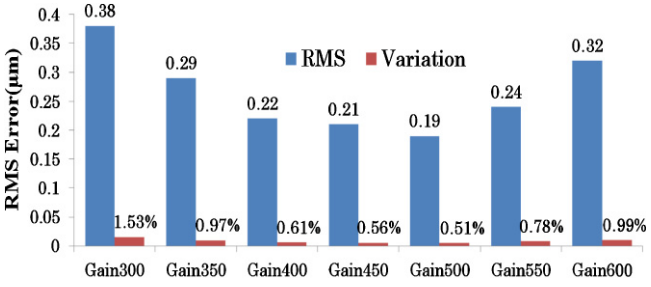

Fig. 5. (Color online) RMS error and peak power variation as a function of gains.

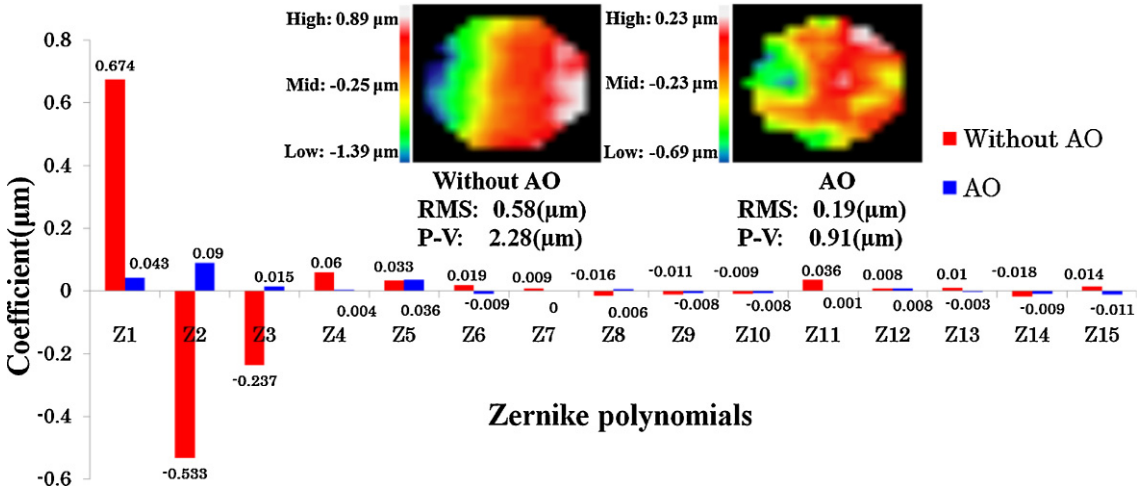

Fig. 6. (Color online) Zernike coefficient values for 15th polynomials with and without AO aberration corrections under dynamic fluid turbulence. The insets show wavefront maps for responses with and without AO, respectively.

Table 2. AO correction results.

	R_a (μm)			
	0.02	0.05	0.32	0.55
Corrected peak power of V_2	20.9621	14.9721	8.2379	7.0246
R_a II′ [Eq. (3)]	0.0191	0.0539	0.3405	0.5567
Relative error %	4.66	7.74	6.39	1.21

Note: R_a II′ are the estimated value of R_a by Eq. (3).

(R_a) errors between static ($V = 0$) and calculated ones for specimens roughness ranging from 0.02 to 0.55 μm are less than 7.74%.

4. Conclusions

An experimental investigation of a flowing fluid layer on metal surface and aberrations correction using adaptive optics system has been studied in this paper. The experimental results show that surface roughness measurement by the optical scattering method will be inevitably affected by the presence of a flowing fluid layer, and after using the adaptive optics system to compensate the optical aberrations, it can significantly improve the attenuation of scattered laser power. The maximum relative error of the estimated roughness R_a by trend equation $Y = 5.8101X^{-0.324}$ is less than 7.8%. The corrected wavefront RMS error is well below 0.2 μm, which demonstrates a good optical system.

Acknowledgement

This work was supported by the National Science Council of Taiwan under Contract No. NSC 102-2221-E-008-067.

References

1) C. Rao, L. Zhu, X. Rao, C. Guan, D. Chen, J. Lin, and Z. Liu: Chin. Opt. Lett. **8** (2010) 966.
2) J. Aceituno, S. F. Sanchez, J. L. Ortiz, and F. J. Aceituno: Publ. Astron. Soc. Pac. **122** (2010) 924.
3) B. Yang, D. Yang, P. Xu, Y. Cao, Z. Feng, and G. Meng: Sens. Actuators A **179** (2012) 193.
4) K. Ogando, N. La Forgia, J. J. Zárate, and H. Pastoriza: Sens. Actuators A **183** (2012) 95.
5) G. Shi, Y. Dai, L. Wang, Z. Ding, and X. Rao, and Y. Zhang: Chin. Opt. Lett. **6** (2008) 424.
6) C. Cánovas, P. M. Prieto, S. Manzanera, A. Mira, and P. Artal: Opt. Lett. **35** (2010) 196.
7) E. J. Fernández and P. Artal: Appl. Opt. **46** (2007) 6971.
8) K. C. Hsu and Y. K. Fuh: Adv. Mater. Res. **154–155** (2010) 1125.
9) Y.-K. Fuh, K. C. Hsu, and J. R. Fan: Opt. Lasers Eng. **50** (2012) 312.
10) Y. K. Fuh, K. C. Hsu, and J. R. Fan: Opt. Lett. **37** (2012) 848.
11) R. Guo and Z. Tao: Opt. Lasers Eng. **47** (2009) 1205.
12) Y. Gao: Proc. ASPE Am. Soc. Precis. Eng. U.S.A. **1** (2001) 329.
13) Y. Gao and Z. Tao: Proc EUSPEN, 2001, p. 684.
14) R. Guo and Z. Tao: Optik **122** (2011) 1890.
15) R. Guo and Z. Tao: Meas. Sci. Technol. **21** (2010) 075306.
16) H. Y. Kim, Y. F. Shen, and J. H. Ahn: J. Mater. Process. Technol. **130–131** (2002) 662.
17) S. H. Wang, Y. H. Tian, Ch. J. Tay, and Ch. G. Quan: Appl. Opt. **42** (2003) 1318.
18) U. Persson: Measurement **18** (1996) 109.
19) U. Persson: Wear **215** (1998) 54.
20) Throlabs: Adaptive Optics Kits Operating [http://www.thorlabs.hk/Thorcat/18100/18182-D02.pdf].